34th Annual International Conference of the IEEE EMBS
San Diego, California USA, 28 August - 1 September, 2012

Hemodynamic Simulation for Surgical Treatment of Congenital Heart Disease

Y Qian, J L Liu, and J F Liu

Abstract— **Numerical analysis of cardiovascular flow is one of several methods of use for the quantitative evaluation of patient-specific treatments. However, due to the complexity of vascular geometry and flow conditions, the cardiovascular flow simulation continues to be a challenging project. As the flow at the peak of systolic heart beat displayed full turbulence, the congenital heart treatments, Norwood and TCPC procedure, were investigated through the use of computational hemodynamic technology, in the present study. On the other hand, at diastolic period, the flow fell to an almost sedentary state. This indicated that the cardiovascular flow experienced a strange transition of flow from systolic peak to diastole. Thus, in order to accurately simulate this transitional flow, a very small time step was applied in the $k-\varepsilon$ turbulent model calculation. Energy losses (EL), local pressure and wall shear stress were analyzed to estimate the result of clinical treatments. It was found that the value of EL, including the influence of respiration, was 1.5 times higher than the value of EL, disregarding respiratory influences. These results indicated that the hemodynamic outcomes of TCPC treatment are noticeably influenced by respiration. The effect of respiration plays an important role in estimating the results of TCPC treatment and thus should be included as one of the important conditions of computational hemodynamic analysis.**

I. Introduction

Hypoplastic left heart syndrome (HLHS) is a type of serious congenital heart disease (CHD). Patients with HLHS suffer from a small, underdeveloped left ventricle, resulting in a heart that cannot effectively supply enough blood flow to provide for the needs of the body. In order to improve blood circulation, surgery for HLHS has to be carried out at a very early stage. In general, three-stage palliative surgical management for newborns is now widely accepted [1], the Norwood, Glenn, and Fontan procedures [2] (Figure 1).

At first-stage surgery, the Norwood operation plays an important role in the overall treatment of HLHS. It has gained popularity as a means of palliating many lesions by creating new passageways of local blood circulation to and from lungs, thereby circumventing some of the defective areas within the heart. Currently, however, there are no quantitative standards to evaluate and predict the outcome of this therapy. Due to the difficulty of studying the outcome directly in vivo, image-based computational fluid dynamics (CFD) was introduced to simulate the blood flow established during the Norwood operation [3].

Y. Qian is with the Australian School of Advanced Medicine, Macquarie University, NSW 2109, Australia (phone: +61-2-9812-3551; fax: +61-2-9812-3610; e-mail: yi.qian@mq.edu.au).

J.L. Liu and J. F. Liu are with the Affiliated Shanghai Children's Medical Center, Shanghai Jiao-Tong University School of Medicine-, Shanghai, China (e-mail: jinlong_liu_man@163.com and liujinfen2002@yahoo.com).

In the present study, a series of in-vitro verification and validations were carried out, including grid independent and calculation domain influence. The aim of the study was not only to confirm the applicability of the computational hemodynamic analysis system in HLHS surgical optimization, but to disclose the characteristics of local hemodynamics at the area of anastomosis, in order to predict the post-operative outcomes of Norwood and third stage operation TCPC (a type of Fontan procedure) through application of CFD methodologies.

Figure 1. Hypoplastic left heart syndrome and clinical treatment.

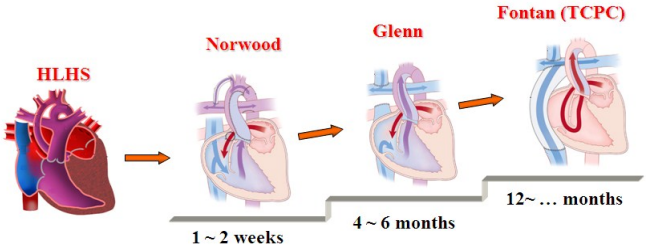

II. Methods

The objective of this study is to investigate the relationship between the characteristics of local hemodynamics at the area of anastomosis, following either Norwood or TCPC operations (patient information was provided by Kitasato University School of Medicine and Shanghai Children's Medical Center) and optimization of the operations for surgical treatment of HLHS, through the use of the computational hemodynamic analysis system developed in our previous studies. This image-based analysis approach employed in the system, involves the following four steps. First, the patient-specific clinical data following operations are acquired by application of medical equipment, including the geometry of the vessels, which will be studied by CT (Computerized Tomography) or MRI (Magnetic resonance imaging) scan, the information of physiologically pulsatile blood flow velocity profiles at the inlets by MRI or Echocardiography, and the distribution of blood pressure at the outlets by catheter with use of pressure sensors. Secondly, the three-dimensional (3-D) geometry of patient-specific vessels are reconstructed from DICOM files, through use of the geometry function within our analysis system, and simultaneously converted into 3-D numerical models [4]. Third, blood flow simulation with the boundary conditions at the inlets and outlets, obtained during the first step, are carried out to acquire a set of converged solutions for the flow field. Last but not least, several methods of visualization and analysis are applied to analyse the hemodynamic properties of blood flow in patient-specific vessels after operations and to give some suggestions and optimization for future treatment.

The Reynolds Number (Re) is expressed by the equation:

$$\mathrm{Re} = \frac{\rho U D}{\mu} \quad (1)$$

where ρ, U, D, and μ are density, velocity, size, and viscosity respectively.

The typical Reynolds number is approximately 4000 within the aorta (Figure 2a), a figure that was calculated through use of an average velocity at the inlet aorta. Thus, turbulence calculation would be utilized in this study. The motion of turbulent fluid can be described by the incorporation of Navier-Stokes (N-S) equations with other turbulent equations.

The energy loss (EL) equation was used to both verify grid independence in the CFD simulation and evaluate the Norwood operation, which is expressed as follows:

$$\mathrm{EL} = \sum_{i}\left(P_i + \frac{1}{2}\rho u_i^2\right)Q_{\mathrm{inlet}} - \sum_{o}\left(P_o + \frac{1}{2}\rho u_o^2\right)Q_o \quad (2)$$

where, P and Q are pressure and flow rate; *i* and o indicate the inlet and outlet.

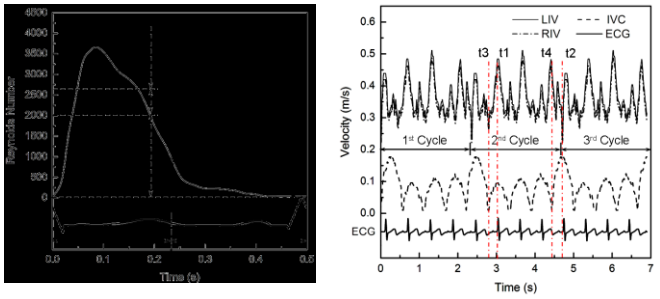

(a) Norwood boundary **(b) TCPC boundary**

Figure 2: Reynolds number and boundary condition *vs*. time

A. Geometry reconstruction

The cross-sectional images in clinic were acquired by use of 16-slice multi-detector row enhanced computerized tomography (CT). The thickness of each slice was 0.625 mm. A series of original cross-sectional CT images was reconstructed, with a non-shrinking smoothing technique employed to generate the numerical model for CFD simulation. Moreover, the accuracy of the reconstructed model had been checked against true geometry with an exacted measurement.

B. Mesh generation

Commercial software, ANSYS®-ICEM 11.0, was applied to the grid generation. In order to accurately measure wall shear stress (WSS) at near-wall-regions, the boundary-fitted hexahedral cell layers were generated at the boundaries to improve the resolution of the relevant scales in fluid motion. In the present study, there were five layers generated with an average nodal space, increasing by a ratio of 1.3. The distance of the first layer to the vessel surface was fixed at 0.01 mm, with the total thickness of the layers changing accordingly with the different branches, ranging from 1.3% to 14.5% depending on the average local-vessel diameters.

Because the accuracy of CFD results relies heavily on both grid resolution and boundary conditions, grid quality tests. Grid independent validation was performed by at the condition of systolic peak. The grid size was maintained at around 1,000,000[3].

C. Boundary conditions

Norwood: The boundary conditions at ascending aorta(AAo), pulmonary artery(PA), coronary artery(CA), descending aorta(DA), and neck vessels (NV), including innominate anonyma (IA), common carotid artery (CCA), and left subclavian artery (SA), were respectively measured in-vivo by using an intracardiac catheter with pressure sensor and echoardiography in real-time with ECG (Electro-cardiogram).

Furthermore, a relatively long length of the inlet blood vessels, extended 20 times of the corresponding vessels' diameter, allowed for the full development of the flow boundary layer at the inlet. The outlet domain for the simulation was likewise extended to be approximately 60-70 times the diameter of its corresponding vessel diameters, sufficiently recovering the blood pressure at the outlet.

TCPC: In order to include the influence from respiration effects on blood distribution in the TCPC simulation, the data measured by patient-specific blood flow through the different frequency of breaths and heart beats was applied at boundary conditions (Figure 2b and Figure 3).

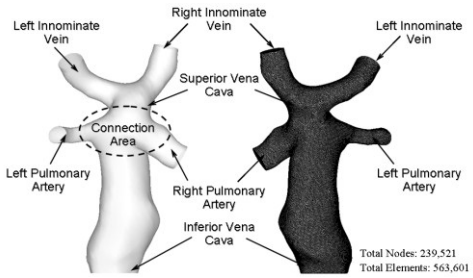

Figure 3: Patient-specific TCPC geometry (left) and Grids (right)

D. Calculation

Transient flow solver was used in the study. The Euler method was applied to solve the time-dependent N-S equations. Flow in the domain was calculated to be mainly associated with turbulence [5]. Due to pulsating flow, the turbulent accelerations results in a higher Re for the transient solution, during systole. Moreover, the accelerating flows result in a larger eddy viscosity than steady flow. This was one of the reasons that simulation appears stable at the systole. On the other hand, performance of simulation during the transition between systole to diastole was predicted to be unstable in nature, due to the deceleration of flow with the reduction of the Re and eddy viscosity [6]. Therefore, it is necessary to estimate a short enough time step in order to catch transient turbulent flows. In the present study, a time step was applied to be =0.00001 s, and each cycle was sub-divided into 50000 time steps (120 BPM). As the convergence criteria, the relative variation of the calculated quantities between two successive iterations was smaller than the pre-assigned maximum residence of 10^{-5}.

The standard $k-\varepsilon$ model with wall-function method was introduced in the turbulent simulation.

III. Results

A. Norwood results

Contour plots of the total pressure and wall shear stress distribution at systolic peak, are illustrated in Figure 4. It can b observed that the total pressure of the blood fluid is high, near the middle position of the aortic arch, whereas a prominent low-pressure area is formed in anastomosis. On the contrary, the distribution of WSS displayed an inverse of characteristics, with relatively high WSS occurring at the AA-PA connection during the whole cycle. Furthermore, the size and location of the low-pressure area and high WSS area are both variable during one cardiac cycle.

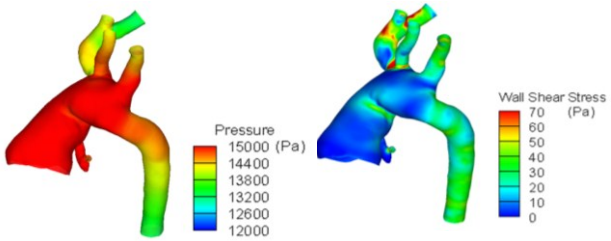

Figure 4. Pressure distribution (left); Wall shear stress (right)

The pressure results were observed to be calculated at the site of AAo, DA, CA and NV, compared with the clinical measurement. The calculated results appear in good agreement with clinical measurements, although there are some differences that are observed at diastolic, starting at the CA sections. These differences may have arisen due to indefinite location during measurement, and may have also been influenced by the inherent dichotomy exhibited by the Valsalva sinus.

The maximum energy loss was approximately 0.146W, a figure which was generated at the systolic peak, whilst the average value of energy loss from pulsatile calculation was 0.0418W. These results were about two times greater than the energy loss calculated by steady calculation.

B. TCPC results

As shown in Figure 5, the total pressure was much higher at the condition that included the influence of breaths and heart beats at t_1, t_3 and t_4, but was significantly lower for pressure distribution. We found relatively lower pressure zones at the left innominate vein (LIV), right innominate vein (RIV), with the size of these zones altered with each subsequent time step. Moreover, time-dependent EL and time-averaged EL were calculated. The EL was lower at the breath including condition (Condition Ⅱ, see figure 2b), whilst the maximum value of time-dependent EL was approximately 0.04725W at Condition Ⅱ, lower than that of the case that did not consider the influence of respiration (Condition Ⅰ), 0.05581W. Furthermore, the time-averaged value of EL at Condition Ⅱ was approximately 1.5 times lower than that of Condition. This implied that the blood flow could obtain energy from respiration to complement the losses induced by flow, confirming the conclusion of the previous study, that spontaneous breathing provided additional energy for blood flow. More specifically, the maximum value of this difference was around 0.05W. Unlike the regular curve shape at Condition, the curve of EL fluctuated at Condition Ⅱ during the entire breath cycle. A big wave followed some small waves (Figure 6), indicating that inspiration and expiration had different influence upon EL. When the patient inspired, the maximum value of EL appeared. From the time-dependent EL, we found some evidence of the influence of respiration on EL.

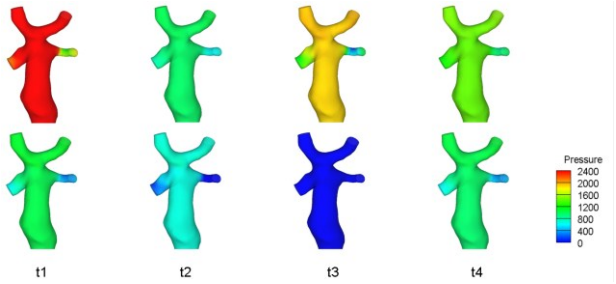

Figure 5. Pressure distribution ; Condition I (top), Condition II (bottom)

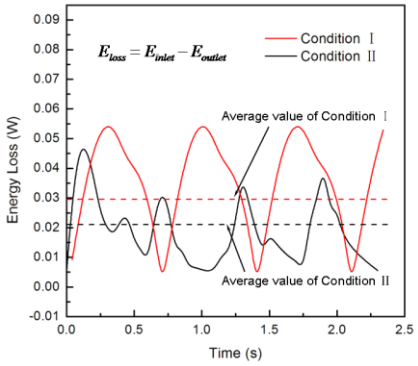

Figure 6. Energy loss (TCPC) by different boundary condition *vs*. time

IV. Discussion

Coupled with the effect of pulsation and downstream branches, the motion of blood flow at the surgical connection area of the PA and AAo became more complicated. Based on the study of Reynolds Number, the blood flow displayed an unusual transition from systolic peak to diastole. The Reynolds Number, served as an indicator for the ration of inertial forces to viscous forces in the flow, decreasing from high value to low level. This suggested that the flow domain was dominant from inertial forces to viscous forces. During this process, small disturbances tend to be amplified.

In this study, the effect of pressure wave reflection was considered by increasing the relative pressure value at the diastole. The heart repeatedly contracted and relaxed in order to carry blood throughout the body. This periodic heartbeat leads to periodic changes in blood pressure in the blood vessels. When the pressure wave coming from the heart (forward running wave) meets the branches of vessels or sudden changes of vascular properties, the reflected wave

(backward-running wave) will be produced. It is estimated that under normal conditions, approximately 80% of the forward running wave is reflected back from arterioles. The geometric configuration of the descending aorta at the level of the renal arterial branches is a very likely site for the production of a major local reflection. The reflected waves have marked physiological importance, increasing pressure in the aortas at the beginning of diastole, thereby improving the coronary perfusion pressure. In this study, the value of relative pressure was raised to imitate the effects of reflected wave at the crossover period of systole and diastole.

Because the TCPC connection area was located in the thoracic cavity and was connected to the lungs through pulmonary arteries, the effect of respiration may have had a significant influence upon the haemodynamic features in the anastomotic region. In the present study, the computational haemodynamic analysis methodology was used to analyze the characteristics of local blood flow by evaluating the influence of respiration in pulsatile simulation. By applying the method, Fast Fourier Transforms, a detailed investigation of respiration effects could be carried out.

Local pressure, WSS, streamlines, EL and flow distribution ratio (FR) at the region of TCPC anastomosis were analyzed by calculations at Condition Ⅰ and Condition Ⅱ. The results showed that the regional flow patterns within the connection area, which was related to the distribution of local pressure, WSS and streamlines, differed from those calculated when the influence of respiration was not taken into account, particularly for the size of low-speed areas and local vortical flow. The spatial conformation of the LIV, created in surgery, led the blood to flow directly into the anterior part of the superior vena cava (SVC), and then into the right pulmonary artery (RPA). Blood flow from the RIV directed to the posterior part of SVC and split into the left pulmonary artery (LPA) and the RPA. The flow from the inferior vena cava (IVC) interacted with that from the LIV and RIV, and then directed into the LPA and RPA. A low velocity flow region existed at the LIV-RIV bifurcation and EL occurred as a result in the area. Moreover, due to the different frequencies between breath and heart beat, the unstable blood flow was shown to be delayed slightly at the IVC at Condition Ⅱ. This could be explained by the delaying of the peak value at the inlet when respiration was taken into account, with respiration changing the pulsatile periodicity of blood flow. Meanwhile, the intensity of vortical flow at the IVC domain was slightly decreased. The salient part generated during surgery near the entrance of the IVC should be the reason as to why a low-speed area and flow recirculation existed in this region.

Compared to the average value of FR at the two conditions at the LPA, no noticeable difference occurred when the influence of respiration was taken into account. Thus, it could be concluded that respiration had little effect on the FR in the patient-specific TCPC study. Whether the influence is universal or not, more patient-specific data is required for examination in future studies. Currently estimation of FR enables the evaluation of the balance of blood flow distribution after Fontan procedures, so as to enhance clinical diagnosis for the long-term post-operative therapies undergone by the patients

The important issue of this study was essential for future correlative studies in the design of Fontan-type procedures. The influence of respiration should be considered, especially in the analysis of local haemodynamic characteristics. To estimate quantitative analysis with greater accuracy and make regional flow features approach the realistic conditions, we advocated that the influence of respiration would better be included in numerical simulations.

V. Conclusion

Based on the analysis of our current study, we effectively validated the ability of a system capable of quantitatively estimating the quality of CHD surgery. Moreover, in-vitro verification and validation processes for grid and boundary condition independents have moreover been carried out. The developed simulation process is also compatible for performance on a personal computer, due to the reduction of grid numbers to an efficient size.

In future studies, a series of before and after cases regarding Norwood surgery will be analyzed, as well as systems to be developed for further stage treatments, both Glenn and Fontan.

Acknowledgment

This study has been supported by Japanese Ministry of Education, Culture, Sports, Science and Technology; grant number A09314800. P.I.: Y. Qian.

References

[1] Norwood WI, Lang P, Casteneda AR and Campbell DN., 1981, “Experience with operations for hypoplastic left heart syndrome”, *J Thorac Cardiovasc Surg*., 82(4), pp.511-519.

[2] Fontan.F. and E. Baudet, 1971, “Surgical repair of tricuspid atresia”. *Thorax*, 26, pp.240-248.

[3] Qian Y, Liu JL, Itatani K and et al, 2010, “Computational hemodynamic analysis in congenital heart disease: simulation of the Norwood procedure”, *Annual of Biomedical Engineering*, 38 (7), pp.2302-2313.

[4] Ku D.N, 1997, “Blood flow on arteries”, *Annual Review of Fluid Mechanics*, 29, pp.399-434.

[5] Taubin G., 1995, “A Signal Processing Approach to Fair Surface Design”, *Proceedings of the 22nd Annual Conference on Computer Graphics and Interactive Techniques*, pp.351-358.

[6] Launder. B.E. and Sharma. B.I., 1974, “Application of the energy dissipation model of turbulence to the calculation of flow near a spinning disc”. Letters in *Heat Mass Transfer*, 1, pp. 131-138.